Structure−Dynamics Coupling between Protein and External Matrix in Sucrose-Coated and in Trehalose-Coated MbCO: An FTIR Study

Sergio Giuffrida, Grazia Cottone, and Lorenzo Cordone*

Istituto Nazionale di Fisica della Materia, Dipartimento di Scienze Fisiche ed Astronomiche, Università di Palermo, Via Archirafi 36 I-90123 Palermo, Italy

Received: May 17, 2004; In Final Form: July 9, 2004

We performed FTIR measurements on carboxy-myoglobin (MbCO) embedded in a sucrose−water matrix to study the degrees of freedom coupling between protein and external matrix in such a system. The work was undertaken on the light of recent results by Giuffrida et al. (*J. Phys. Chem. B* **2003**, *107*, 13211−13217), who evidenced, in trehalose-coated MbCO, a structured water−sugar environment of the protein, tightly coupled to the heme pocket structure. Such information was obtained through a suitable analysis of the temperature dependence of the CO stretching and of the water association bands in samples of different content of residual water. We applied here the same analysis to sucrose-coated MbCO. Comparison between the results obtained in the two saccharide systems points out the different free-energy landscape experienced by the protein and matrix atoms. This is put forward by the differences in heme pocket structure (shape of the CO stretching band) and in protein environment (shape of the water association band). Furthermore, our data evidence a tighter protein−matrix coupling in trehalose than in sucrose. We suggest this difference to be at the basis for the better efficiency, as biopreservant, of trehalose with respect to sucrose, since the appearance of damages on biological structures will more involve structural variations of the surrounding matrix in the former sugar.

1. Introduction

It is well known that biological structures embedded in sugar matrixes can overcome adverse conditions such as dehydration and high temperatures. Under such condition, the interaction with the surrounding saccharide−water matrix causes large hindering of internal dynamics of the embedded structures.[1−9] Among sugars, trehalose (a disaccharide composed of two [1,1]-linked α,α units of glucopyranose) appears the most effective protectant since it gives the best recovery of biomaterials after drying and resuspension. This sugar is present in some organisms that can survive extreme drought and high temperature in the lack of metabolic processes under a condition known as anhydrobiosis. These organisms can long remain under such condition without suffering damages, while following rehydration their vegetative cycle restarts. Large attention has been devoted toward the understanding of the properties that make trehalose unique with respect to other sugars.[10−15] The water replacement hypothesis, formulated on the basis of spectroscopic studies, proposed that trehalose directly binds to biostructures thus replacing water.[16] Other mechanisms have been proposed according to which trehalose entraps water molecules close to the biostructures surface.[17,18] Furthermore, the ability of sugars to form high-viscosity glasses has been suggested to play a relevant role in bioprotection, the efficiency being related to the glass-transition temperature.[19]

With the aim of shedding further light on the origin of the trehalose peculiarity, we performed FTIR measurements on sucrose-coated carboxy-myoglobin and compared the results with the analogous ones already reported for the trehalose-coated protein.[20]

As it is well known, the stretching band of the bound CO in MbCO (Figure 1) is split into three different sub-bands. These bands reflect the taxonomic A substates,[21] which correspond to three specific different environments experienced by the bound CO within the heme pocket.[22] The relative intensity of these sub-bands depends on external parameters such as pH, temperature, and pressure.[23−25] The thermal behavior of the above band therefore gives information on the thermal interconversion among taxonomic and lower hierarchy substates, which are evidenced, for example, by the thermal line broadening and peak frequency shifts.

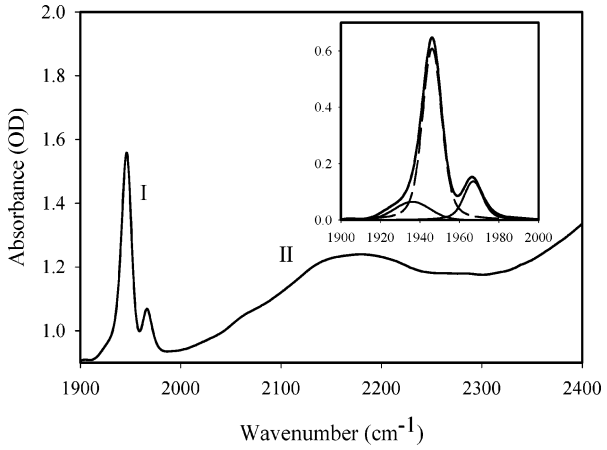

Figure 1. CO stretching band (I, 1900−2000 cm^{-1}) and association band of water (II, 2000−2400 cm^{-1}) in trehalose-coated MbCO (sample 3_T, see Materials and Methods) at 20 K.[20] The inset shows the fitting of the CO band in terms of three taxonomic A substates.[21]

As Figure 1 shows, on the high-frequency side of the CO stretching band appears the water association band, which is attributed to a combination of the bending mode of water molecules with intermolecular vibrational modes.[26] This band is absent in anhydrous saccharide samples; moreover, in the

* Corresponding author. E-mail: cordone@fisica.unipa.it.

10.1021/jp047894k CCC: $27.50
Published on Web 08/31/2004

TABLE 1: Estimate of the Sample Water Content (OD cm^{-1}) in Sucrose-Coated and Trehalose-Coated MbCO at 300 K

	overdry samples		dry samples		hydrated samples	
	sample 1_S	sample 1_T[a]	sample 2_S	sample 2_T	sample 3_S	sample 3_T
estimate from the water association band	3.9	5.5	9.6	7.6	35.1	31.5
estimate from the water combination band	0.2	0.2	3.3	1.2	19.3	18.0

[a] Data on trehalose-coated MbCO are taken from ref 20.

presence of suitable solutes, coupling of the bending modes of water molecules with intermolecular vibrational modes, involving nonwater H-bonding groups, may also contribute to the band.[20]

Librizzi et al.[27] observed a strict correlation between the thermal evolution (263−323 K) of the CO stretching band and the thermal evolution of the water association band in samples of MbCO embedded in trehalose matrixes of different hydration. The study was extended to a wider temperature range (20−300 K) by Giuffrida et al.,[20] who reported on the existence, in trehalose-coated MbCO, of a structured environment of the protein, tightly coupled to the heme pocket structure. Such information was obtained by analyzing, for both the CO stretching and water association bands, the spectra distance (SD) of the various normalized spectra from the respective normalized spectrum measured at 20 K. This is defined as[20]

$$\mathrm{SD} = \{\int_\nu [A(\nu,T) - A(\nu,T = 20\ \mathrm{K})]^2 \mathrm{d}\nu\}^{1/2} \approx \{\sum_\nu [A(\nu,T) - A(\nu,T = 20\ \mathrm{K})]^2 \Delta\nu\}^{1/2} \quad (1)$$

where $A(\nu)$ is the normalized absorbance at frequency ν and $\Delta\nu$ is the frequency resolution. The above quantity represents the deviation of the normalized spectrum at temperature T from the normalized spectrum at 20 K. For the protein, it reflects the overall thermally induced heme pocket structural rearrangements evidenced by the changes in the relative population of taxonomic (A) and lower hierarchy substates. Moreover, in view of the structured profile of the water association band, it was assumed[20] that the SD relative to this last band reflects thermally induced structural rearrangements of the water dipoles network within our samples. Accordingly, our analysis gave information on the coupling between temperature-induced rearrangements of the heme pocket and of the structured saccharide−water environment. Such coupling resulted different in sucrose with respect to trehalose.

The shapes of both the CO stretching band and of the water association band depend on sample composition (sugar, buffer, salts, amount of sodium dithionite, etc.). For this reason, we compared samples of sucrose-coated with samples of trehalose-coated MbCO, which were prepared starting from solution of identical composition, differing only for the kind of sugar employed.

2. Materials and Methods

Lyophilized ferric horse myoglobin was purchased from Sigma (Sigma, St. Louis, MO) and used without further purification. Sucrose from Fluka (Buchs, CH, Biochemical grade >99.5%) was used without purification. For preparation of samples of sucrose-coated MbCO, ferric myoglobin was dissolved ($\sim 5 \times 10^{-3}$ M) in a solution containing 2×10^{-1} M sucrose and 2×10^{-2} M phosphate buffer (pH 7 in water). The solution was equilibrated with CO and reduced by anaerobic addition of sodium dithionite (10^{-1} M). Aliquots (0.1 mL) of the above solution were layered on CaF_2 windows of ~ 1 cm^2 surface. All samples were initially dried for ~8 h under a CO atmosphere in a silica gel desiccator. Further drying proceeded at 353 K: 1 h at ambient pressure and ~15 h under vacuum. Samples containing various amounts of residual water were then prepared following a procedure analogous to the one used for trehalose-coated MbCO.[20]

The driest sample studied (1_S) (where the subscript S stands for sucrose) was—after drying at 353 K—immediately put into the sample holder and transferred into the cryostat where it was left open to allow further drying under vacuum at 353 K. Drying ended after ~3.5 h, when the water content estimated through the area under the band at ~5200 cm^{-1} was comparable to the area of the analogous sample of trehalose-coated MbCO.[20] The reason for choosing the combination band at ~5200 cm^{-1} for estimating the water content will be discussed below (see discussion of Table 1). Because of the slower water release by the sucrose sample,[28] longer drying at 353 K within the cryostat is needed in sucrose than in trehalose[20] for obtaining the same water content. Measurements on sample 1_S were then performed in the temperature interval 350−20 K.

A second sample (2_S) was—after drying at 353 K—exposed ~3 min to room moisture at 300 K, before putting it into the sample holder. The sample was then confined by putting a Teflon O-ring and a second CaF_2 window on top of it, to avoid water release during measurements, and transferred into the cryostat where it was left ~2 h, at room temperature, before starting measurements. This allowed diffusion of the absorbed water. Measurements were then performed in the temperature interval 300−20 K.

A further sample (3_S) was—after drying at 353 K—overnight equilibrated in the presence of 60% relative humidity at 300 K. The sample was then put into the holder and confined by putting a Teflon O-ring and a second CaF_2 window on top of it, to avoid water evaporation, and then transferred into the cryostat. Measurements were performed in the temperature interval 300−20 K. After hydration, the sample was not dipping and remained hard enough to stay in a vertical position.

After the above high-temperature treatments, all samples remained in an amorphous state as evidenced by the very low turbidity detected by measuring the absorbance at 1900 cm^{-1} at 300 K.[28]

Measurements of optical absorption and circular dichroism spectroscopy showed that almost full recovery was obtained when redissolving the samples after drying in the desiccator, before heating at 353 K under vacuum. Lower recovery ≥85% was obtained after the high-temperature treatment. Such treatment was necessary for having samples of similar thermal history, starting from extremely dry ones. The recovery was slightly better (at the limit of the error) in the trehalose (see also the Discussion section). In this respect, the water uptake by dried samples makes the shape of the CO stretching band to progressively evolve toward the one of a nontreated protein in aqueous solution, thus indicating that damaged protein barely contributes to the signal we analyze. To evidence eventual temperature-induced degradation of our disaccharides, we performed a qualitative analysis (Barfoed essay) that showed

the complete absence of reducing monosaccharides, even in the sucrose sample, following the drying and heating procedure.

Water content was contemporary estimated either by measuring (in OD × cm^{-1}) the overall area under the profile of the association band (see Figure 4

, upper panels) or by measuring the area delimited by the tangent between the two minima to the profile of the water band at ∼5200 cm^{-1}. We remind that the last band is an intramolecular one, ascribed to a combination of water bending with asymmetric stretching.[26,29,30] The estimate of residual water obtained by the two methods will be reported and discussed in the next section (see Table 1).

All FTIR measurements were performed on a Jasco 410 FTIR spectrometer with 2 cm^{-1} resolution. The cryostat and the temperature control used were, respectively, Optistat CF-V and ITC-503, from Oxford Instruments Ltd., U.K.

The stretching band of the bound CO (1900−2000 cm^{-1}) is usually fitted in terms of the three A substates;[21] at variance, suitable fitting in sucrose-coated MbCO could be obtained only considering the presence of four taxonomic (A) substates (see below). A Gaussian extrapolation took into account the queue of the association band in the range 1900−2000 cm^{-1}. The fitting of the water association band was performed in terms of Gaussian or Voigtian components, which were dependent on the sample humidity. A Gaussian extrapolation took into account the queue of the adjacent higher frequency bands (ν > 2400 cm^{-1}). The above fitting gave the areas under the absorption profiles that were used for normalization of the raw spectra, after subtraction of the extrapolation. The error bar shown in the plots of SD versus temperature (Figures 5−7) represents the maximum SD differences obtained in two different measurements on overdry samples, which are the only ones for which the water content could be exactly reproduced. Indeed, only for such samples the water content was measured during the drying procedure, within the cryostat, under vacuum, at 353 K. The same error bar has been assumed also for less dry samples for which the water content can be barely tuned.

As already mentioned in the Introduction, we compare here samples of sucrose-coated with samples of trehalose-coated protein, which were prepared from solution of identical composition, differing only for the kind of sugar employed.

Our samples contained very high protein concentration; this was necessary since the protein−matrix coupling becomes increasingly detectable by increasing the MbCO concentration. Indeed, the matrix is fully *imprinted* only in the presence of confluent protein−trehalose−water structures.

3. Results and Discussion

3.1 Samples Water Content. In Table 1, we report the samples water content estimated (at 300 K) by measuring both the area under the profile of the association band or the area delimited by the tangent between the two minima to the profile of the water combination band at ∼5200 cm^{-1}. In the same table are also shown data reported for similar samples of trehalose-coated MbCO;[20] such samples from now on will be called 1_T, 2_T, and 3_T.

As mentioned in the Introduction, contributions to the water association band may arise either from combination of the bending mode of water molecules with intermolecular water−water vibrational modes[26] or from combinations of the bending mode of water molecules with intermolecular vibrations involving nonwater hydrogen bond forming groups.[20] Accordingly, two "sub-populations" of absorbers contribute to the band. This makes the area under the association band depend linearly on water concentration only in two extreme cases: (i) in water-rich systems, that is, when water−water interaction dominates the band and (ii) when the band is dominated by the interaction between water molecules and nonwater H-bond forming groups. At variance, the above area must have a nonlinear dependence on water concentration when both water−water interaction and interaction between water molecules and nonwater H-bond forming groups contribute to the band. Further contribution to the above nonlinearity could also arise from the presence of the different sub-bands in the structured profile of the water association band (see Figure 4). Indeed, the plausible variation of relative weight and oscillator strength of such sub-bands, upon drying the saccharide-containing matrixes, could also contribute to a nonlinear dependence of the area underlying the association band on water concentration.

At variance from the association band, the water combination band at ∼5200 cm^{-1} is due to intramolecular processes, that is, to absorption by single water molecules. This band, therefore, gives a less biased estimate of the sample water content. In this case, nonlinearity on the water content, by drying, may only be brought about by variations of the band oscillator strength, because of the number and strength of hydrogen bonds in which water molecules are involved.

From the above observations, it follows that the ratio W_A/W_C (where W_A and W_C are the estimates of water content from the water association band and from the water combination band, respectively) will not depend on water content only in the two extreme cases in which only one of the two sub-populations of absorbers contributes to the water association band. In particular, under the naive assumption that each water molecule contributes one oscillator when coupled to a nonwater H-bond forming group (case a) and 1/2 oscillator when coupled to a water molecule (case b), one will have $(W_A/W_C)_S \approx (W_A/W_C)_T = K$ for case a, that is, overdry systems, or $K/2$ for case b, that is, water-rich samples.

On the basis of this observation, we obtained information on the relative weight of the above sub-populations, in the association band in the two sugar systems, by considering the following ratio:

$$R = (W_A/W_C)_S/(W_A/W_C)_T$$

This ratio must be unity, independent of water concentration, when the two sugars exhibit identical hydrogen-bonding capability. At variance, for sugars having different potential to form hydrogen bonds, the R value will approach unity in particular for the two cases a and b described above.

Exploiting the above ratio R enables to get preliminary information on the origin of the differences between the sucrose and the trehalose systems reported in Table 1:

(i) for the overdry samples 1_S and 1_T the R value (0.7) indicates that a slightly larger fraction of the area under the association band is contributed by water−water interactions in sucrose than in trehalose. This result is consistent with the larger number of intramolecular hydrogen bonds present in sucrose with respect to trehalose, which leaves, in the sugar molecule, a lower number of sites available to hydrogen bond with water;[31]

(ii) for the intermediate samples 2_S and 2_T in which, according to the estimate through the water combination band (nonbiased), the water content is sizably different, the value of the ratio R is about 0.5;

(iii) for the water-rich samples 3_S and 3_T a much lower discrepancy between the two estimates ($R \approx 1.0$) is present since bulklike water−water interactions essentially dominate the band.

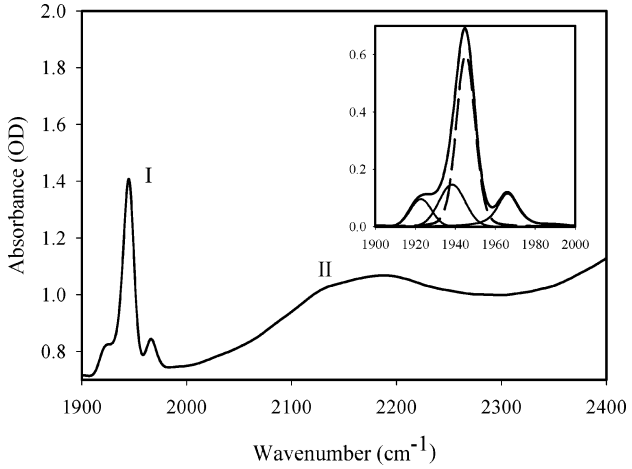

Figure 2. CO stretching band (I, 1900−2000 cm^{-1}) and association band of water (II, 2000−2400 cm^{-1}) in sucrose-coated MbCO (sample 3_S, see Materials and Methods) at 20 K. The inset shows the fitting of the CO band in terms of four taxonomic substates.

The above points confirm the expected behavior of the quantity *R* discussed above and in agreement with previous data in the literature[31−33] indicate that water−sugar interactions are stronger in trehalose than in sucrose samples.

3.2 CO Stretching and Water Association Bands. Figure 2 shows the spectrum of sucrose-coated MbCO in the region 1900−2400 cm^{-1}, at 20 K. As evident, four substates are needed for a suitable fitting of the stretching band of the bound CO.

In Figure 3 are shown the bands of CO stretching at 20 and 300 K of sucrose-coated (upper panel) and of trehalose-coated MbCO[20] (lower panel), as obtained after extraction from the raw data and normalization. We deal with normalized spectra since we are interested in changes of the absorption profile, which reflect heme pocket conformational rearrangements. Normalized absorption profiles of the water association band at 20 and 300 K, as obtained after extraction from the raw data and normalization, are shown in the upper and lower panels of Figure 4 for the two systems, respectively. Again, we deal here with normalized spectra since we are interested in variations of the band structure, which contain information on structural rearrangements of the water dipoles network, irrespective of the band oscillator strength.

As evident, IR spectra of both bound CO and of water association band are different in the two sugar systems at all the hydration levels analyzed. In particular, concerning the heme pocket structure, four sub-bands are needed for fitting the CO stretching in sucrose, while in trehalose, as usual, three A substates are sufficient (see the insets in Figures 1, 2).

The room-temperature spectrum of the CO stretching band in MbCO embedded in a sucrose matrix was already reported by Librizzi et al.[28] who obtained a suitable fitting of the band in terms of only three substates. In the present work, we have been forced to fit the CO band in terms of four sub-bands since fitting in terms of only three substates resulted in very low quality for the low-temperature spectra. Moreover, fitting in terms of four substates sizably increases the fitting quality for high-temperature spectra. The fourth substate can barely be thought to be the one formerly reported[21] as A_2, since its peak frequency at room temperature is 1927 cm^{-1}, while the A_2 peak frequency is 1942 cm^{-1}.

Concerning the external matrix, as evidenced by the structure of water association band, comparison of the two sugar systems shows larger differences between extra dry and dry samples than between humid samples. This is expected on the basis of the considerations on the parameter *R*, reported in the preceding section. The above conclusions are further strengthened when analyzing the fittings on the band in Figure 4 in terms of the sum of Gaussian or Voigtian components (work in progress).

Figure 5 shows the spectra distances (see eq 1) of the CO stretching and of water association bands (respectively, SD_{CO} and SD_{WATER}), referred to the spectrum at 20 K, in the sucrose system. As evident, the extremely dry sample 1_S has the lowest temperature induced variations in the whole temperature range, both for the matrix and the protein, while more hydrated samples result dependent on temperature at ∼50 K. Furthermore,

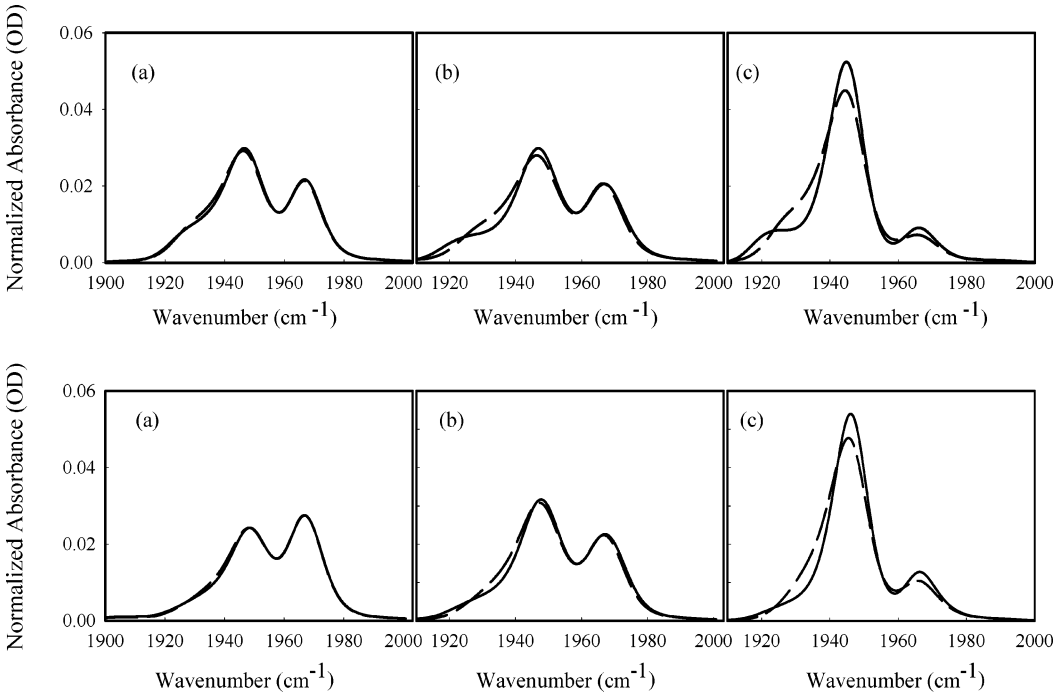

Figure 3. Normalized spectra of the CO stretching band at 20 K (solid lines) and 300 K (short dash lines) in sucrose-coated (upper panels) and trehalose-coated MbCO[20] (lower panels). (a) samples 1_S and 1_T; (b) 2_S and 2_T; (c) 3_S and 3_T.

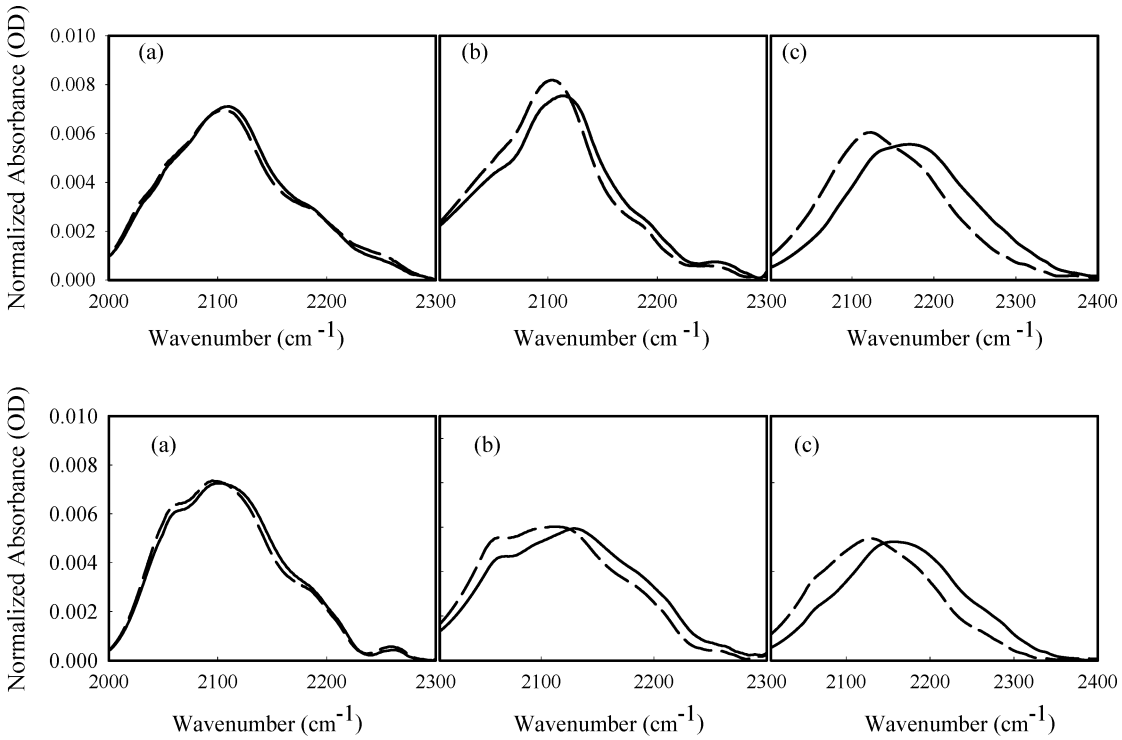

Figure 4. Normalized spectra of the water association band at 20 K (solid lines) and 300 K (short dash lines) in the sucrose (upper panels) and in the trehalose system (lower panels) 12. (a) samples 1_S and 1_T; (b) 2_S and 2_T; (c) 3_S and 3_T.

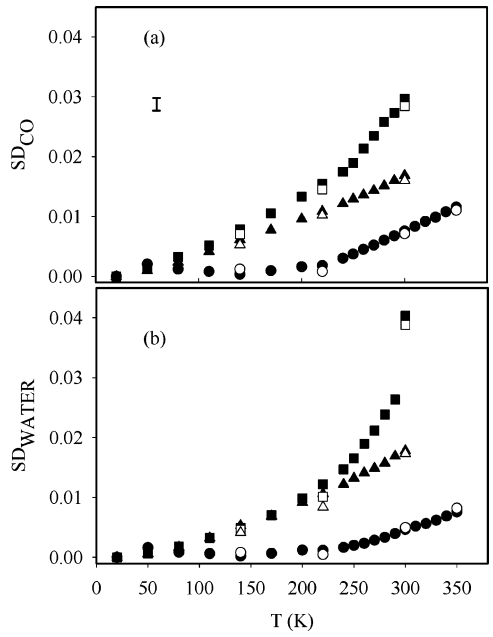

Figure 5. (a) CO stretching band spectra distance (SD_{CO}) referred to the spectrum measured at 20 K vs temperature in the sucrose-coated MbCO; (b) Water association band spectra distance (SD_{WATER}) referred to the spectrum measured at 20 K vs temperature, in the sucrose matrixes. Circles: sample 1_S; triangles: sample 2_S; squares: sample 3_S. Full symbols: data points obtained during cooling; open symbols: data points obtained during heating. Error bar calculated on the basis of SD reproducibility in overdry samples (see Materials and Methods) is shown.

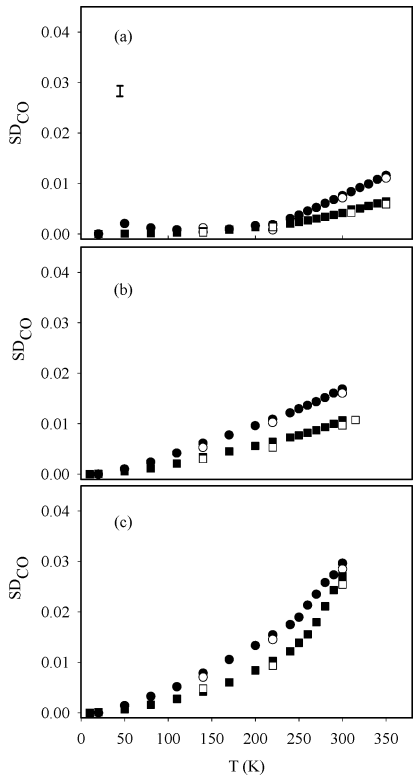

Figure 6. CO stretching band spectra distance (SD_{CO}) referred to the spectrum measured at 20 K vs temperature. (a) sample 1_S (circles) and sample 1_T (squares); (b) sample 2_S and 2_T; (c) sample 3_S and sample 3_T. Full symbols: data points obtained during cooling; open symbols: data points obtained during heating. Data on trehalose-coated MbCO are taken from ref 20.

SD_{WATER} for these last samples result in coincidence up to ∼180 K and exhibit larger increase in the water richer sample 3_S at higher temperature. We attribute this behavior to the presence of weakly bound, bulklike water molecules present in this sample above ∼180 K, which break the long-range structural (and dynamic) correlation in the water dipole network. In this respect, ∼180 K is, recurrently, the temperature at which the so-called dynamic transition has been observed in experimental and simulative studies, in protein−water systems.[34−37] At variance, a comparison of the SD_{CO} of samples 2_S and 3_S shows

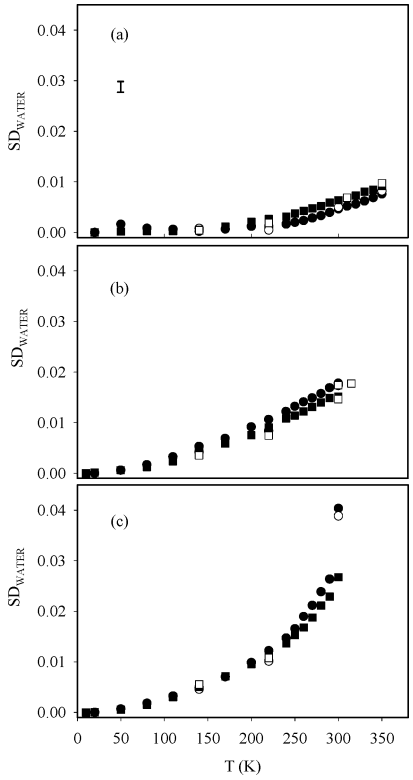

Figure 7. Water association band spectra distance (SD_{WATER}) referred to the spectrum measured at 20 K vs temperature. (a) sample 1_S (circles) and sample 1_T (squares); (b) sample 2_S and 2_T; (c) sample 3_S and sample 3_T. Full symbols: data points obtained during cooling; open symbols: data points obtained during heating. Data on trehalose-coated MbCO are taken from ref 20.

that slightly larger temperature induced structural variations take place in sample 3_S already at 140 K. This behavior is indicative of a larger amount of internal processes taking place in a rigid environment not involving displacements of the protein surface[38,39] in sample 3_S than in sample 2_S, already at 140 K.

As reported by Giuffrida et al.,[40] comparison between the SD_{CO} thermal evolution (Figure 5a) and analogous plots, in which the iron atom[7,34] or hydrogen atoms mean square displacements[8,35] are reported, evidences how the thermal evolution of equilibrium structures (conformational substates) strictly parallels the thermal evolution of mean square displacements of different atoms, measured on different time scales. This unambiguously shows that the amplitude increase of mean square fluctuations, which takes place above $\sim$ 180 K, stems from interconversion among high hierarchy conformational substates, as up to now assumed.

Detailed information on the different behavior of the sucrose and trehalose systems is obtained by analyzing the data in Figures 6 and 7, where are reported, superimposed, the SD_{CO} and SD_{WATER} relative to sucrose and to trehalose samples.[20]

As evident, the external matrixes exhibit very similar thermal behavior in samples 1_S, 2_S, 3_S and 1_T, 2_T, 3_T, respectively. Interestingly, this holds true for samples 2_S and 2_T, notwithstanding the sizable difference in water content. At variance, comparison of the SD_{CO} in the two sugar systems evidences systematically larger heme pocket thermal induced structural rearrangements in sucrose than in trehalose, thus implying larger heme pocket motional freedom in the former sugar with respect to the latter. This finding indicates a looser coupling of the degrees of freedom of the protein to the degrees of freedom of the external matrix, in sucrose than in trehalose, plausibly involved in the better bioprotection of the latter saccharide.

Opposite conclusion on the protein−matrix coupling could be reached by considering the appearance of a fourth substate in sucrose-coated MbCO; indeed, stronger coupling could lead to stronger structural constraints for the protein, resulting in the appearance of a new substate. In this respect, the structure of a protein and its internal dynamics are described through a 3*N*-3 dimension energy landscape, where *N* is the number of atoms in the protein and its surroundings, whose interaction with the protein is not vanishing.[40,41] Accordingly, the fourth substate present in sucrose and not in trehalose-coated MbCO stems from different protein surroundings, which produce a different energy landscape. This does not imply that the protein structure must slavishly follow the structural rearrangements of the matrix.

As reported in the Material and Methods section, no large difference in recovery is obtained when redissolving MbCO, which has been embedded either in trehalose or in sucrose matrixes. It must be considered, however, that myoglobin is a very stiff protein, while the superiority of trehalose among carbohydrates for preservation of biological structures is well known and established.[10−15,42] Furthermore, recent results evidenced loss of functional recovery (paralleled by loss of pheophytin) following sucrose coating for the Reaction Center of Rhodobacter Sphaeroides (RC) (work in progress), which, at variance, is very well recovered following trehalose coating.[29,30] Loss of functional protein, again paralleled by loss of pheophytin, takes place when RC is dried in the absence of saccharides,[29] to a larger extent than in sucrose-coated protein.

4. Conclusions

Comparison of the present FTIR results on sucrose-coated MbCO samples with previous ones on trehalose-coated protein[20] evidences the different shapes of the CO stretching and water association bands, which are, respectively, signatures of the energy landscape experienced by protein atoms and by water molecules in the two systems. In particular, a fourth taxonomic A substate, which is absent in trehalose, appears in sucrose.

The thermal behavior of the spectra distances (dynamics) points out that in both sugar systems the extent of thermal rearrangements of the external matrix is in the whole analogous in overdry, dry, and humidified samples. At variance, larger thermally induced heme pocket rearrangements take place in sucrose than in trehalose, thus indicating a looser protein−matrix coupling in the former system, arising from a different hydrogen bond network in the protein−water−sugar structures.[18] This, in turn, must be reflected in a lower coupling between the dynamics of the protein and the dielectric properties of the matrix.[43]

In conclusion, our results suggest that trehalose organizes a friendly sugar−water environment in which native biological structures are better entrapped. Indeed, because of the tight coupling, the appearance of structural damages is a rare event, since it strongly involves the surrounding matrix.

The reported results shed light toward the understanding, at microscopic level, of the origin of the trehalose peculiarity and, in particular, suggest why carbohydrates that have potential to form hydrogen bonds exhibit different capability in preserving biomaterials.[44,45]

Acknowledgment. We wish to thank Prof. G. Ciccotti and Prof. G. Venturoli for useful discussions.

References and Notes

(1) Hagen, S. J.; Hofrichter, J.; Eaton, W. A. *Science* **1995**, *269*, 959−962.

(2) Gottfried, D. S.; Peterson, E. S.; Sheikh, A. G.; Wang, J.; Yang, M.; Friedman, J. M. *J. Phys. Chem.* **1996**, *100*, 12034−12042.
(3) Kleinert, T.; Doster, W.; Leyser, H.; Petry, W.; Schwarz, V.; Settles, M. *Biochemistry* **1998**, *37*, 717−733.
(4) Lichtenegger, H.; Doster, W.; Kleinert, T.; Birk, A.; Sepiol, B.; Vogl, G. *Biophys. J.* **1999**, *76*, 414−422.
(5) Rector, D.; Jiang, J.; Berg, M. A.; Fayer, M. D. *J. Phys. Chem. B* **2001**, *105*, 1081−1092.
(6) Dantsker, D.; Samuni, U.; Friedman, A. J.; Yang, M.; Ray, A.; Friedman, J. M. *J. Mol. Biol.* **2002**, *315*, 239−251.
(7) Cordone, L., Galajda, P.; Vitrano, E.; Gassmann, A.; Ostermann, A.; Parak, F. *Eur. Biophys. J.* **1998**, *27*, 173−176.
(8) Cordone, L.; Ferrand, M.; Vitrano, E.; Zaccai, G. *Biophys. J.* **1999**, *76*, 1043−1047.
(9) Cottone, G.; Cordone, L.; Ciccotti, G. *Biophys. J.* **2001**, *80*, 931−938
(10) Crowe, J. H.; Crowe, L. M. *Science* **1984**, *223*, 701−703.
(11) Bianchi, G.; Gamba, A.; Murellie, C.; Salamini, F.; Bartels, D. *Plant J.* **1991**, *1*, 355−359.
(12) Uritani, M.; Takai, M.; Yoshinaga, K. *J. Biochem.* **1995**, *117*, 774−779.
(13) Panek, A. D. *Braz. J. Med. Biol. Res.* **1995**, *28*, 169−181.
(14) Crowe, L. M. *Comp. Biochem. Physiol., A* **2002**, *131*, 505−513.
(15) Zayed, G.; Roos, Y. *Proc. Biochem.* **2004**, *39*, 1081−1086.
(16) Carpenter, J. F.; Crowe, J. H. *Biochemistry* **1989**, *28*, 3916−3922.
(17) Belton, P. S.; Gil, A. M. *Biopolymers* **1994**, *34*, 957−961.
(18) Cottone, G.; Ciccotti, G.; Cordone, L. *J. Chem. Phys.* **2002**, *117*, 9862−9866.
(19) Green, J. L.; Angell, C. A. *J. Phys. Chem.* **1989**, *93*, 2880−2882.
(20) Giuffrida, S.; Cottone, G.; Librizzi, F.; Cordone, L. *J. Phys. Chem. B* **2003**, *107*, 13211−13217.
(21) Frauenfelder, H.; Parak, F.; Young, R. D. *Annu. Rev. Biophys. Chem.* **1988**, *17*, 451−479.
(22) Vojtechovsky, J.; Chu, K.; Berendzen, J.; Sweet, R. M.; Schlichting, I. *Biophys. J.* **1999**, *77*, 2153-2174.
(23) Makinen, M. W.; Houtchens, R. A.; Caughey, W. S. *Proc. Natl. Acad. Sci. U.S.A.* **1979**, *76*, 6042−6046.
(24) Beece, D.; Eisenstein, L.; Frauenfelder, H.; Good, D.; Marden, M. C.; Reinisch, L.; Reynolds, A. H.; Sorensen, L. B.; Yue, K. T. *Biochemistry* **1980**, *19*, 5147−5157.
(25) Frauenfelder, H.; Alberding, N. A.; Ansari, A.; Braunstein, D.; Cowen, B. R.; Hong, M. K.; Iben, I. E. T.; Johnson, J. B.; Luck, S.; Marden, M. C.; Mourant, J. R. *J. Phys. Chem.* **1990**, *94*, 1024−1037.
(26) Eisenberg, D.; Kauzmann, W. *The Structure and Properties of Water*; Oxford University Press: London, 1969.
(27) Librizzi, F.; Viappiani, C.; Abbruzzetti, S.; Cordone, L. *J. Chem. Phys.* **2002**, *116*, 1193−1200.
(28) Librizzi, F.; Vitrano, E.; Cordone, L. *Biophys. J.* **1999**, *76*, 2727−2734.
(29) Palazzo, G.; Mallardi, A.; Hochkoeppler, A.; Cordone, L.; Venturoli, G. *Biophys. J.* **2002**, *82*, 558−568.
(30) Francia, F.; Palazzo, G.; Mallardi, A.; Cordone, L.; Venturoli, G. *Biophys. J.* **2003**, *85*, 1043−1047.
(31) Ekdawi-Sever, N. C.; Conrad, P. B.; de Pablo, J. J. *J. Phys. Chem. A* **2001**, *105*, 734−742.
(32) Branca, C.; Magazù, S.; Maisano, G.; Migliardo, P. *J. Chem. Phys.* **1999**, *111*, 281−287.
(33) Magazù, S.; Maisano, G.; Migliardo, P.; Mondelli, C. *Biophys. J.* **2004**, *86*, 3241−3249.
(34) Parak, F.; Knapp, E. W.; Kucheida, D. *J. Mol. Biol.* **1982**, *161*, 177−194.
(35) Doster, W.; Cusak, S.; Petry, W. *Nature* **1989**, *337*, 754−756.
(36) Steinbach, P. J.; Loncharich, R. J.; Brooks, B. R. *Chem. Phys.* **1991**, *158*, 383−394.
(37) Pal, S. K.; Peon, J.; Zewail, A. H. *Proc. Natl. Acad. Sci. U.S.A.* **2002**, *99*, 1763−1768.
(38) Rector, D.; Jiang, J.; Berg, M. A.; Fayer, M. D. *J. Phys. Chem. B* **2001**, *105*, 1081−1092.
(39) Weik, M.; Ravelli, R. B. G.; Silman, I.; Sussman, J. L.; Gros, P.; Kroon, J. *Protein Sci.* **2001**, *10*, 1953−1961.
(40) Giuffrida, S.; Cottone, G.; Librizzi, F.; Cordone, L. In *Progress in Condensed Matter Physics: Festschrift in honour of Vincenzo Grasso*; Mondio, G., Sipigni, L., Eds.; Messina, SIF: Bologna, Italy, 2004; pp 131−138.
(41) Frauenfelder, H.; Fenimore, P. W.; McMahon, B. H. *Biophys. Chem.* **2002**, *98*, 35-48.
(42) Leslie, S. B.; Israeli, E.; Lighthart, B.; Crowe, J. H.; Crowe, L. M. *Appl. Environ. Microbiol.* **1995**, *61*, 3592−3597.
(43) Fenimore, P. W.; Frauenfelder, H.; McMahon, B. H.; Parak, F. *Proc. Natl. Acad. Sci. U.S.A.* **2002**, *99*, 16047−16051.
(44) Crowe, J. H.; Crowe, L. M.; Jackson, S. A. *Arch. Biochem. Biophys.* **1983**, *220*, 615−617.
(45) Arakawa, T.; Pretrelski, S. J.; Kennedy, W. C.; Carpenter, J. F. *Adv. Drug Delivery Rev.* **1993**, *10*, 1−28.